

Field angle-dependent thermal conductivity in nodal superconductors

T. R. Abu Alrub and S. H. Curnoe

*Department of Physics and Physical Oceanography,
Memorial University of Newfoundland, St. John's, NL, A1B 3X7, Canada*

We apply a semi-classical method to the problem of field angle-dependent oscillations of the density of states and thermal conductivity for nodal superconductors and apply our results to the superconductor $\text{PrOs}_4\text{Sb}_{12}$. The oscillatory contributions to the thermal conductivity for all possible point node configurations for a superconductor with T_h symmetry are calculated. It is found that experimental results are best accounted for by nodes in the off-axis directions $[\pm \sin \phi_0, 0, \pm \cos \phi_0]$, which are associated with the time-reversal breaking, triplet paired phase with symmetry $D_2(E)$.

PACS numbers: 74.20.-z, 71.27.+a, 71.10.-w

I. INTRODUCTION

The low temperature thermodynamic properties of unconventional superconductors are governed by nodal quasiparticles. In the presence of a small magnetic field $H_{c1} \leq H \ll H_{c2}$, it was shown by Volovik¹ that the dominant contribution to the density of states (DOS) for superconductors with line nodes comes from delocalised quasiparticles, in contrast to s -wave superconductors in which the DOS is dominated by quasiparticles localised inside vortex cores.^{1,2} Volovik argued that the delocalised states experience a semi-classical adjustment to their energy due to the magnetic field which is expressed as a Doppler shift $\omega \rightarrow \omega - \mathbf{v}_s(\mathbf{r}) \cdot \mathbf{k}$, where $\mathbf{v}_s(\mathbf{r}) = \frac{1}{2m\mathbf{r}}\hat{\beta}$ is the superfluid velocity and β is the winding angle around a single vortex. As a result, contributions proportional to the magnetic field have been predicted to appear in thermodynamic and transport properties of line node superconductors^{1,3,4,5,6,7,8,9,10,11}.

Magnetic contributions that appear because of the Doppler shift will strongly depend on the position of the magnetic field with respect to the nodes. Consequently, oscillations in the DOS and related quantities have been predicted for superconductors with line nodes in a rotating magnetic field,^{5,12,13,14,15,16,17,18,19,20,21,22,23} and have been observed experimentally in in-plane thermal conductivity in $\text{YBa}_2\text{Cu}_3\text{O}_7$.^{24,25} Similar results have been found for other unconventional superconductors,^{26,27,28,29,30,31,32} including $\text{YNi}_2\text{B}_2\text{C}$ ²⁹ and $\text{PrOs}_4\text{Sb}_{12}$,³⁰ which are reported to have point nodes instead of line nodes. Oscillations in the angular field dependence of the specific heat have also been observed in several unconventional superconductors.^{33,34,35,36,37,38,39,40}

Volovik's proof that, in superconductors with line nodes, delocalised quasi-particles have a greater contribution to the low-energy DOS than vortex localised quasiparticles does not extend to superconductors with point nodes. However, we are interested in finding the oscillatory component of the DOS in a rotating magnetic field, for which the semi-classical method, applied to delocalised quasi-particles, may be valid. For delocalised states, oscillations are obtained just by Doppler-shifting

the quasiparticle energies. For localised states, the amplitude of oscillations may be found by calculating separately the DOS for the case when the field points in the direction of the nodes and the case when the field is perpendicular to the nodes and subtracting the results for the two cases. The former case corresponds to the s -wave result, which gives the contribution from localised quasi-particles as $N_{s-\text{loc.}} \sim N_F \xi^2 / R^2 \sim N_F H / H_{c2}$, where ξ is the coherence length and R is the inter-vortex spacing. This sets a lower bound on the DOS contributions from localised quasi-particles in superconductors with line nodes or point nodes. The upper bound of the DOS contribution from localised quasiparticles in superconductors with nodes is found when the field is parallel to the nodes. Volovik found that for superconductors with line nodes, the localised quasiparticles contribute $N_{\text{line-loc.}} \sim N_F \sqrt{H/H_{c2}} / \log \sqrt{H_{c2}/H}$ which he found to be less than the delocalised contribution $N_{\text{line-deloc.}} \sim N_F \sqrt{H/H_{c2}}$. The oscillatory contribution for the delocalised states is contained within $N_{\text{line-deloc.}}$, while the oscillation amplitude for the localised states is $\sim N_{\text{line-loc.}} - N_{s-\text{loc.}} \approx N_{\text{line-loc.}}$. Thus the DOS oscillations in a line node superconductor are dominated by the delocalised contribution, and the semi-classical treatment is valid. For a point node superconductor, one finds that the delocalised contribution is $N_{\text{point-deloc.}} \sim N_{\text{point-loc.}} \sim N_{s-\text{loc.}}$. Again, the oscillatory contribution for delocalised states is contained within $N_{\text{point-deloc.}}$ while the oscillation amplitude for the localised states is found by comparing $N_{\text{point-loc.}}$ to $N_{s-\text{loc.}}$. This suggests that while both localised and delocalised states contribute to the DOS in point node superconductors, the oscillatory component is dominated by the delocalised states. We will assume that this is the case, but a more thorough investigation of the role of vortex localised quasiparticles in point node superconductors is warranted.

Field dependent thermal conductivity measurements are usually performed in one of two experimental configurations. In layered compounds in which the c -axis conductivity is low, such as in $\text{YBa}_2\text{Cu}_3\text{O}_7$, the in-plane conductivity is usually measured with the B-field rotating in the same plane. Then one in-plane component of

the current will be parallel to vortices produced by the B-field while the other in-plane component of the current is perpendicular to the vortices. This introduces complications when calculating the different components of the current averaged over the vortex lattice, since a different kind of averaging procedure should be used depending on whether the heat current is parallel or perpendicular to the vortices.⁷ As a consequence, for a field rotating in the xy plane, in-plane components of the conductivity will oscillate with a period of twice the field angle even when there are no nodes at all, and this oscillation will dominate any nodal contribution.^{32,63} Thus, whenever possible, the preferred set-up is to measure the heat currents perpendicular to the rotating B-field.³²

In the superconductor $\text{PrOs}_4\text{Sb}_{12}$, the pairing symmetry is widely thought to be unconventional,^{30,41,42,43,44,45,46,47,48,49} with spin triplet pairing⁴⁸ and broken time reversal symmetry.⁴¹ Power law behavior has been observed in many thermodynamic and transport measurements at low temperature,^{30,43,44,47,49} which suggests the existence of nodes in the gap function; however a nodeless gap function has been observed in some experiments.^{50,51,52,53} Oscillations of the thermal conductivity in a rotating magnetic field are another indication that there are nodes in the gap function.³⁰ In previous works,^{54,55} we have attempted to determine the symmetry of the superconducting state in $\text{PrOs}_4\text{Sb}_{12}$ using available experimental results. Among the various possible choices, we selected the spin triplet paired states belonging to the three dimensional irreducible representation T_u of the point group T_h with symmetry $D_2(C_2) \times \mathcal{K}$ and order parameter components $(0,0,1)$ and $D_2(E)$ with components $(i|\eta_2|, 0, |\eta_1|)$. We label these phases ‘A’ and ‘B’ respectively. The A phase is unitary, and has two cusp point nodes in the directions $\pm[0, 0, 1]$, while the B phase is nonunitary and has four cusp point nodes in the directions $[\pm \sin \phi_0, 0, \pm \cos \phi_0]$, where ϕ_0 is an angle determined from phenomenological parameters.⁵⁵ We will consider these and all other symmetry-allowed phases with point nodes.

In this article we calculate the DOS and residual transport under an applied magnetic field. We consider both the clean and dirty limits, in which the impurity scattering rate is much smaller or greater than the Doppler shift, respectively. For the purpose of comparison, we begin by stating in Section II results for the residual DOS and thermal conductivity for the d -wave (line node) superconductors. Section III is devoted to point nodes applied to $\text{PrOs}_4\text{Sb}_{12}$. In Section IV we compare our results to experiment. Concluding remarks are made in Section V.

II. DENSITY OF STATES AND THERMAL CONDUCTIVITY FOR SUPERCONDUCTORS WITH LINE NODES

In this section we consider a d -wave superconductor (such as $\text{YBa}_2\text{Cu}_3\text{O}_7$) with line nodes along the directions $k_x = \pm k_y$ and a magnetic field applied in the $k_x k_y$ -plane at an angle ϵ with respect to the x axis. In the vicinity of a node, the gap function takes the form $\Delta(\mathbf{k}) \approx v_g k_2$, where k_2 points perpendicular to the node in the xy -plane and $\mathbf{v}_g = \frac{\partial \Delta(\mathbf{k})}{\partial \mathbf{k}} \Big|_{\text{node}}$ is the gap velocity. The quasiparticle energy is $E(\mathbf{k}) = \sqrt{\epsilon^2(\mathbf{k}) + \Delta^2(\mathbf{k})} \approx \sqrt{v_F^2 k_1^2 + v_g^2 k_2^2}$, where k_1 points in the direction of the node. Thus, in the vicinity of a node, the Green’s function takes the form

$$G(\mathbf{k}, i\tilde{\omega}_n, \mathbf{r}) = \frac{i\tilde{\omega}_n + \alpha_j(\mathbf{r}) + v_F k_1}{(i\tilde{\omega}_n + \alpha_j(\mathbf{r}))^2 + v_F^2 k_1^2 + v_g^2 k_2^2} \quad (1)$$

where $i\tilde{\omega}_n = i\omega_n + i\Gamma_0$, $\alpha_j(\mathbf{r}) = \mathbf{v}_s(\mathbf{r}) \cdot \mathbf{k}_{Fj}$ is the Doppler shift at the j th node and $\Gamma_0 = -\Im \Sigma_{ret}(\omega = 0)$ is the scattering rate at zero energy. The self-energy Σ is derived from the T-matrix formalism for impurity scattering and is the solution to the self-consistent equation^{5,56}

$$\Sigma(i\omega_n) = \frac{\Gamma G_0(i\tilde{\omega}_n, \mathbf{r})}{c^2 - G_0^2(i\tilde{\omega}_n, \mathbf{r})} \quad (2)$$

where Γ is proportional to the impurity concentration, c is related to the phase shift δ_0 , $c = \cot \delta_0$ and

$$G_0(i\tilde{\omega}_n, \mathbf{r}) = \frac{1}{\pi N_F} \sum_{\mathbf{k}} G(\mathbf{k}, i\tilde{\omega}_n, \mathbf{r}). \quad (3)$$

N_F is the density of states at the Fermi surface. In the unitary limit ($c = 0$) this yields a self-consistent equation for the scattering rate^{7,57}

$$\Gamma_0^2 = \pi^2 N_F v_F v_g \Gamma \left[\ln \left(\frac{p_0^2}{\sqrt{(\alpha_1^2(\mathbf{r}) + \Gamma_0^2)(\alpha_2^2(\mathbf{r}) + \Gamma_0^2)}} \right) + \frac{\alpha_1(\mathbf{r})}{\Gamma_0} \tan^{-1} \left(\frac{\alpha_1(\mathbf{r})}{\Gamma_0} \right) + \frac{\alpha_2(\mathbf{r})}{\Gamma_0} \tan^{-1} \left(\frac{\alpha_2(\mathbf{r})}{\Gamma_0} \right) \right]^{-1}. \quad (4)$$

where p_0 is a cutoff and $\alpha_{1,2}(\mathbf{r})$ are the Doppler shifts at two opposite nodes and can be written as

$$\alpha_1(\mathbf{r}) = \frac{k_F}{2mr} \sin \beta \sin(\pi/4 - \epsilon) \quad (5)$$

$$\alpha_2(\mathbf{r}) = \frac{k_F}{2mr} \sin \beta \cos(\pi/4 - \epsilon) \quad (6)$$

where r is the distance from the centre of the vortex core, β is the vortex winding angle and ϵ is the angle of the magnetic field relative to the x -axis.

A. Density of States

The DOS is given by

$$-N(\omega, \mathbf{r}) = \frac{1}{\pi} \int \frac{d^3 k}{(2\pi)^3} \Im G_{ret}(\mathbf{k}, \omega, \mathbf{r}) \quad (7)$$

where the integral over \mathbf{k} is evaluated as the sum of four separate volume integrations centred about each node.⁵⁹ Then the DOS at the Fermi energy is

$$N(0, \mathbf{r}) = \frac{\Gamma_0}{\pi^2 v_F v_g} \left[\ln \left(\frac{p_0^2}{\sqrt{(\alpha_1^2(\mathbf{r}) + \Gamma_0^2)(\alpha_2^2(\mathbf{r}) + \Gamma_0^2)}} \right) + \frac{\alpha_1(\mathbf{r})}{\Gamma_0} \tan^{-1} \left(\frac{\alpha_1(\mathbf{r})}{\Gamma_0} \right) + \frac{\alpha_2(\mathbf{r})}{\Gamma_0} \tan^{-1} \left(\frac{\alpha_2(\mathbf{r})}{\Gamma_0} \right) \right] \quad (8)$$

In the clean limit $(\Gamma_0/|\alpha(\mathbf{r})|) \rightarrow 0$ and

$$N(0, \mathbf{r}) \approx \frac{|\alpha_1(\mathbf{r})| + |\alpha_2(\mathbf{r})|}{2\pi v_F v_g} \quad (9)$$

$$= \frac{k_F}{2mr} |\sin \beta| \frac{\max[|\sin \epsilon|, |\cos \epsilon|]}{2\sqrt{2}\pi v_F v_g}. \quad (10)$$

This result necessarily has the same form as the finite frequency DOS $N(\omega) \sim |\omega|$ of superconductor with line nodes. Averaging over the vortex unit cell we obtain the result as in Ref. 12,

$$\langle N(0, \mathbf{r}) \rangle_H = \frac{1}{\pi R^2} \int_{\xi_0}^R dr r \int_0^{2\pi} d\beta N(0, \mathbf{r}) \quad (11)$$

$$\sim N_F \frac{\xi_0}{R} \max[|\sin \epsilon|, |\cos \epsilon|] \quad (12)$$

where $\frac{\xi_0}{R} \sim \sqrt{\frac{H}{H_{c2}}}$. Evidently, there are four-fold oscillations in the DOS as a function of the field angle ϵ .

In the dirty limit $|\alpha(\mathbf{r})|/\Gamma_0 \ll 1$ we find

$$N(0, \mathbf{r}) = \frac{\Gamma_0}{\pi^2 v_F v_g} \left[2 \ln \left(\frac{p_0}{\Gamma_0} \right) + \frac{\alpha_1^2(\mathbf{r}) + \alpha_2^2(\mathbf{r})}{\Gamma_0^2} \right]. \quad (13)$$

The first term is just the impurity induced DOS $N(0)$,⁵⁹ so

$$\delta N(0, \mathbf{r}) = N(0, \mathbf{r}) - N(0) = \frac{1}{4\pi^2 r^2} \frac{v_F}{v_g \Gamma_0} \sin^2 \beta \quad (14)$$

and the average DOS is⁶

$$\langle \delta N(0, \mathbf{r}) \rangle_H \sim N_F \frac{\Delta_0}{\Gamma_0} \frac{H}{H_{c2}} \ln \left(\frac{H_{c2}}{H} \right). \quad (15)$$

where $\Delta_0 = \frac{v_F}{\xi_0} \sim N_F v_F v_g$. In this case, impurities remove the field directional dependence of the DOS.

B. Thermal conductivity

The thermal conductivity tensor is defined by the Kubo formula.⁵⁸ In the limit $T \rightarrow 0$ it is expressed in terms of the imaginary part of the Green's function as^{59,60}

$$\frac{\tilde{\kappa}(0, \mathbf{r})}{T} = \frac{k_B^2}{3} \sum_{\mathbf{k}} \mathbf{v}_F \mathbf{v}_F \text{Tr}[\Im \tilde{G}_{ret}(0, \mathbf{r}) \Im \tilde{G}_{ret}(0, \mathbf{r})], \quad (16)$$

where k_B is the Boltzmann constant and \mathbf{v}_F is the Fermi velocity in the direction of \mathbf{k} . By again dividing the integration over \mathbf{k} into regions centred over each node, this eventually leads to

$$\frac{\tilde{\kappa}(0, \mathbf{r})}{T} = \frac{k_B^2}{3} \frac{\sum_{j=1}^4 \mathbf{v}_F \mathbf{v}_F}{(2\pi)^2 v_F v_g} \int_0^{2\pi} d\theta \int_0^{p_0} dp p \times \frac{2\Gamma_0^2}{[(\alpha_j(\mathbf{r}) + p)^2 + \Gamma_0^2]^2} \quad (17)$$

where the integration variable is $p = \sqrt{v_F^2 k_1^2 + v_g^2 k_2^2}$. Performing the integration yields

$$\frac{\tilde{\kappa}(0, \mathbf{r})}{T} = \frac{k_B^2}{3} \frac{\sum_{j=1}^4 \mathbf{v}_F \mathbf{v}_F}{\pi v_F v_g} \left(1 + \frac{\alpha_j(\mathbf{r})}{\Gamma_0} \left[\tan^{-1} \left(\frac{\alpha_j(\mathbf{r})}{\Gamma_0} \right) - \frac{\pi}{2} \right] \right) \quad (18)$$

where now \mathbf{v}_F is evaluated at each node. Summing over nodes yields

$$\frac{\delta \tilde{\kappa}(0, \mathbf{r})}{T} = \frac{\tilde{\kappa}(0, \mathbf{r}) - \tilde{\kappa}(0, 0)}{T} = \frac{k_B^2}{6\pi} \frac{v_F}{v_g} \times \left(\frac{\alpha_1(\mathbf{r})}{\Gamma_0} \tan^{-1} \left(\frac{\alpha_1(\mathbf{r})}{\Gamma_0} \right) + \frac{\alpha_2(\mathbf{r})}{\Gamma_0} \tan^{-1} \left(\frac{\alpha_2(\mathbf{r})}{\Gamma_0} \right) - \frac{\alpha_1(\mathbf{r})}{\Gamma_0} \tan^{-1} \left(\frac{\alpha_1(\mathbf{r})}{\Gamma_0} \right) - \frac{\alpha_2(\mathbf{r})}{\Gamma_0} \tan^{-1} \left(\frac{\alpha_2(\mathbf{r})}{\Gamma_0} \right) \right) \quad (19)$$

In the clean limit $\alpha(\mathbf{r}) \gg \Gamma_0$, the thermal conductivity is

$$\frac{\delta \tilde{\kappa}(0, \mathbf{r})}{T} = \frac{k_B^2}{12} \frac{v_F}{v_g} \left(\frac{|\alpha_1(\mathbf{r})| + |\alpha_2(\mathbf{r})|}{\Gamma_0} - \frac{|\alpha_1(\mathbf{r})| - |\alpha_2(\mathbf{r})|}{\Gamma_0} \right), \quad (20)$$

and the average over the vortex unit cell is

$$\left\langle \frac{\delta\tilde{\kappa}(0, \mathbf{r})}{T} \right\rangle_H \sim k_B^2 \frac{v_F}{v_g} \frac{\Delta_0}{\Gamma_0} \sqrt{\frac{H}{H_{c2}}} \left(\begin{array}{cc} \frac{1}{\sqrt{2}} \max[|\sin \epsilon|, |\cos \epsilon|] & |\sin(\pi/4 - \epsilon)| - |\cos(\pi/4 - \epsilon)| \\ |\sin(\pi/4 - \epsilon)| - |\cos(\pi/4 - \epsilon)| & \frac{1}{\sqrt{2}} \max[|\sin \epsilon|, |\cos \epsilon|] \end{array} \right). \quad (21)$$

In the dirty limit $\alpha(\mathbf{r}) \ll \Gamma_0$ we find

$$\frac{\delta\tilde{\kappa}(0, \mathbf{r})}{T} = \frac{k_B^2}{6\pi} \frac{v_F}{v_g} \left(\begin{array}{cc} \frac{\alpha_1^2(\mathbf{r}) + \alpha_2^2(\mathbf{r})}{\Gamma_0^2} & \frac{\alpha_1^2(\mathbf{r}) - \alpha_2^2(\mathbf{r})}{\Gamma_0^2} \\ \frac{\alpha_1^2(\mathbf{r}) - \alpha_2^2(\mathbf{r})}{\Gamma_0^2} & \frac{\alpha_1^2(\mathbf{r}) + \alpha_2^2(\mathbf{r})}{\Gamma_0^2} \end{array} \right) \quad (22)$$

The average over the vortex unit cell is

$$\left\langle \frac{\delta\tilde{\kappa}(0, \mathbf{r})}{T} \right\rangle_H \sim k_B^2 \frac{v_F}{v_g} \frac{\Delta_0^2}{\Gamma_0^2} \frac{H}{H_{c2}} \ln \left(\frac{H_{c2}}{H} \right) \left(\begin{array}{cc} 1 & -\sin 2\epsilon \\ -\sin 2\epsilon & 1 \end{array} \right) \quad (23)$$

Thus, as in the DOS, impurities remove oscillations due to nodes in the diagonal components of the thermal conductivity.

III. DENSITY OF STATES AND THERMAL CONDUCTIVITY FOR A POINT NODE SUPERCONDUCTOR

We will first assume that there are an arbitrary number of *linear* (*i.e.* vanishing linearly with momentum) point nodes in the gap function, and that the gap velocities v_g are equal and isotropic around each node. We begin by finding a self-consistent equation for the scattering rate Γ_0 analogous to Eq. 4. For point nodes, Eq. 3 is

$$G_0(0, \mathbf{r}) = \frac{1}{\pi N_F} \frac{\sum_{\text{nodes}}}{(2\pi)^3 v_F v_g^2} \int_0^{2\pi} d\phi \int_0^\pi d\theta \sin \theta \int_0^{p_0} dp p^2 \times \frac{-\alpha_j(\mathbf{r}) + i\Gamma_0 + p \cos \theta}{(-\alpha_j(\mathbf{r}) + i\Gamma_0)^2 - p^2} \quad (24)$$

where the integration variable is $p = \sqrt{v_F^2 k_1^2 + v_g^2 (k_2^2 + k_3^2)}$ and k_1 is parallel to the node while $k_{2,3}$ are perpendicular to the node. In Eq. 24, we have again divided the volume of integration into parts each centred around a node. The integrations yield

$$G_0(0, \mathbf{r}) = \frac{-i}{N_F 2\pi^3 v_F v_g^2} \sum_{\text{nodes}} \left[(\Gamma_0 + i\alpha_j(\mathbf{r})) p_0 - \frac{\pi}{2} (\Gamma_0 + i\alpha_j(\mathbf{r}))^2 \right]. \quad (25)$$

Now we assume that there are four nodes which occur in pairs on opposite sides of the Fermi surface. Partners in each pair produce equal and opposite Doppler shifts.

Summing over nodes we find

$$G_0(0, \mathbf{r}) = \frac{-i}{N_F 2\pi^3 v_F v_g^2} \left[4p_0 \Gamma_0 + \pi(\alpha_1^2(\mathbf{r}) + \alpha_2^2(\mathbf{r}) - 2\Gamma_0^2) \right] \equiv \frac{\Gamma}{i\Gamma_0} \quad (26)$$

This result can easily be generalized to include more pairs of nodes. Equating the imaginary parts of (26) yields the self-consistent equation for the scattering rate Γ_0 ,

$$\Gamma_0 = \frac{\pi^3}{2} \frac{N_F v_F v_g^2 \Gamma}{p_0 \Gamma_0 - \frac{\pi}{2} \Gamma_0^2 + \frac{\pi}{4} (\alpha_1^2(\mathbf{r}) + \alpha_2^2(\mathbf{r}))}. \quad (27)$$

This equation describes how the scattering rate due to impurities is modified in the presence of Doppler shifted quasiparticles.

As in Section II, we will assume that the magnetic field is parallel to the xy -plane with an angle ϵ from the x axis,

$$\mathbf{H} = H(\cos \epsilon \hat{x} + \sin \epsilon \hat{y}). \quad (28)$$

The supercurrent is

$$\mathbf{v}_s(\mathbf{r}) = \frac{1}{2mr} (-\sin \epsilon \cos \beta \hat{x} + \cos \epsilon \cos \beta \hat{y} + \sin \beta \hat{z}). \quad (29)$$

For now we will assume that all pairs of nodes are in the xy -plane at the positions

$$\mathbf{k}_{F1} = \pm k_F (\cos \phi_0 \hat{x} - \sin \phi_0 \hat{y}) \quad (30)$$

$$\mathbf{k}_{F2} = \pm k_F (\cos \phi_0 \hat{x} + \sin \phi_0 \hat{y}). \quad (31)$$

The angle ϕ_0 is zero in the A phase of $\text{PrOs}_4\text{Sb}_{12}$ (and the gap function is doubly degenerate) and $\phi_0 \neq 0$ in the B phase. This corresponds to the choice of the domain $(1, 0, 0)$ of the A phase and the domain $(|\eta_1|, i|\eta_2|, 0)$ of the B phase. In each phase, two other domains are possible and these will be discussed in the next section.

The Doppler shifts are

$$\alpha_1(\mathbf{r}) = \pm \mathbf{v}_s(\mathbf{r}) \cdot \mathbf{k}_{F1} = \pm \frac{k_F}{2mr} \cos \beta [-\sin \phi_0 \cos \epsilon - \cos \phi_0 \sin \epsilon] \quad (32)$$

$$\alpha_2(\mathbf{r}) = \pm \mathbf{v}_s(\mathbf{r}) \cdot \mathbf{k}_{F2} = \pm \frac{k_F}{2mr} \cos \beta [\sin \phi_0 \cos \epsilon - \cos \phi_0 \sin \epsilon] \quad (33)$$

The following averages over the vortex unit cell will be useful:

$$\begin{aligned} \langle \alpha_1^2(\mathbf{r}) + \alpha_2^2(\mathbf{r}) \rangle_H &\sim \frac{v_F^2}{R^2} \ln \left(\frac{R}{\xi_0} \right) [\cos^2 \phi_0 \sin^2 \epsilon + \sin^2 \phi_0 \cos^2 \epsilon] \\ \langle \alpha_1^2(\mathbf{r}) - \alpha_2^2(\mathbf{r}) \rangle_H &\sim \frac{v_F^2}{R^2} \ln \left(\frac{R}{\xi_0} \right) \sin 2\phi_0 \sin 2\epsilon. \end{aligned} \quad (34)$$

A. Density of states

The DOS is given by Eq. 7. Using (3) and (26) we find

$$N(0, \mathbf{r}) = \frac{2\Gamma_0^2}{\pi^3 v_F v_g^2} \left[\frac{p_0}{\Gamma_0} - \tan^{-1} \left(\frac{p_0}{\Gamma_0} \right) + \frac{\alpha_1^2(\mathbf{r}) + \alpha_2^2(\mathbf{r})}{2\Gamma_0^2} \tan^{-1} \left(\frac{p_0}{\Gamma_0} \right) \right]. \quad (35)$$

In zero magnetic field we retain our previous result for the impurity induced density of states⁶⁰, then the magnetic contribution is

$$\delta N(0, \mathbf{r}) \approx \frac{\alpha_1^2(\mathbf{r}) + \alpha_2^2(\mathbf{r})}{2\pi^2 v_F v_g^2} \quad (36)$$

which depends upon the Doppler shifts to the same power as that of the frequency in the low frequency DOS in zero magnetic field, $N(\omega) \sim \omega^2$ for superconductors with point nodes. Taking the average over the vortex unit cell, we get

$$\frac{\langle \delta N(0, \mathbf{r}) \rangle_H}{N_F} \sim \frac{H}{H_{c2}} \ln \left(\frac{H_{c2}}{H} \right) [\cos^2 \phi_0 \sin^2 \epsilon + \sin^2 \phi_0 \cos^2 \epsilon]. \quad (37)$$

Thus we find that the DOS oscillates with rotating magnetic field as $\cos 2\epsilon$ and is universal *i.e.* independent of the scattering rate.

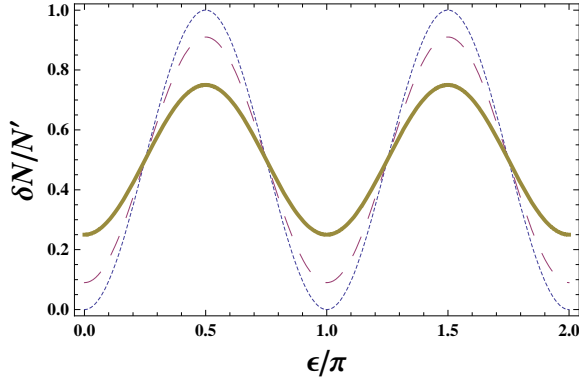


FIG. 1: (Color online) Oscillations in the density of states (Eq. 37) for different values of ϕ_0 as a function of the field angle ϵ . The dotted line is for $\phi_0 = 0$ (A phase), the dashed line for $\phi_0 = \arcsin(0.3)$ and the bold line for $\phi_0 = \frac{\pi}{6}$. $N' \sim N_F \frac{H}{H_{c2}} \ln \left(\frac{H_{c2}}{H} \right)$.

B. Thermal Conductivity

Beginning with Eq. 16, we divide the volume of integration into parts centred around each node,

$$\frac{\tilde{\kappa}(0, \mathbf{r})}{T} = \frac{k_B^2}{3} \frac{\sum_{j=1}^4 \mathbf{v}_F \mathbf{v}_F}{(2\pi)^3 v_F v_g^2} \int_0^{2\pi} d\phi \int_0^\pi d\theta \sin \theta \int_0^{p_0} dp p^2 \frac{\Gamma_0^2}{[(\alpha_j(\mathbf{r}) + p)^2 + \Gamma_0^2]^2} \quad (38)$$

where the integration variable is again $p = \sqrt{v_F^2 k_1^2 + v_g^2 (k_2^2 + k_3^2)}$. The integrations yield

$$\frac{\tilde{\kappa}(0, \mathbf{r})}{T} = \frac{k_B^2}{12\pi^2} \frac{\sum_{j=1}^4 \mathbf{v}_F \mathbf{v}_F}{v_F v_g^2} \left[\frac{\Gamma_0^2 + \alpha_j^2(\mathbf{r})}{\Gamma_0} \right] \times \left[\frac{\pi}{2} - \tan^{-1} \frac{\alpha_j(\mathbf{r})}{\Gamma_0} - \frac{\alpha_j(\mathbf{r})\Gamma_0}{\alpha_j^2(\mathbf{r}) + \Gamma_0^2} \right] \quad (39)$$

where again our previously derived expression for the residual conductivity in zero magnetic field⁶⁰ is recovered. The matrix $\mathbf{v}_F \mathbf{v}_F$ for one node is equal to the contribution for the node on the opposite side of the Fermi surface, but $\alpha_j(\mathbf{r})$ changes sign at opposite nodes, therefore terms which are odd in $\alpha_j(\mathbf{r})$ will vanish. The sum over nodes yields (keeping only the magnetic part)

$$\begin{aligned} \frac{\delta \tilde{\kappa}(0, \mathbf{r})}{T} &= \frac{k_B^2}{12\pi} \frac{1}{v_F v_g^2 \Gamma_0} [\alpha_1^2(\mathbf{r})(\mathbf{v}_F \mathbf{v}_F)_1 + \alpha_2^2(\mathbf{r})(\mathbf{v}_F \mathbf{v}_F)_2] \\ &= \frac{k_B^2}{12\pi} \frac{v_F}{v_g^2 \Gamma_0} \begin{pmatrix} (\alpha_1^2(\mathbf{r}) + \alpha_2^2(\mathbf{r})) \cos^2 \phi_0 & \frac{1}{2}(\alpha_2^2(\mathbf{r}) - \alpha_1^2(\mathbf{r})) \sin 2\phi_0 & 0 \\ \frac{1}{2}(\alpha_2^2(\mathbf{r}) - \alpha_1^2(\mathbf{r})) \sin 2\phi_0 & (\alpha_1^2(\mathbf{r}) + \alpha_2^2(\mathbf{r})) \sin^2 \phi_0 & 0 \\ 0 & 0 & 0 \end{pmatrix}. \end{aligned} \quad (40)$$

Finally we perform the average over the vortex unit cell,

$$\left\langle \frac{\delta \tilde{\kappa}(0, \mathbf{r})}{T} \right\rangle_H \sim k_B^2 \frac{v_F \Delta_0^2}{v_g^2 \Gamma_0} \frac{H}{H_{c2}} \ln \left(\frac{H_{c2}}{H} \right) \begin{pmatrix} \cos^2 \phi_0 [\cos^2 \phi_0 \sin^2 \epsilon + \sin^2 \phi_0 \cos^2 \epsilon] & -\frac{1}{4} \sin 2\phi_0 \sin 2\epsilon & 0 \\ -\frac{1}{4} \sin 2\phi_0 \sin 2\epsilon & \sin^2 \phi_0 [\cos^2 \phi_0 \sin^2 \epsilon + \sin^2 \phi_0 \cos^2 \epsilon] & 0 \\ 0 & 0 & 0 \end{pmatrix} \quad (41)$$

where $\Delta_0^2 = \frac{v_F^2}{\xi_0^2} \sim N_F v_F v_g^2$. The A phase of $\text{PrOs}_4\text{Sb}_{12}$ corresponds to $\phi_0 = 0$, and the only component of the thermal conductivity which is non-vanishing is $\kappa_{xx} \sim \sin^2 \epsilon$.

Other domains

The phase $D_2(E)$ has two other nodal configurations,⁶⁴ which may be found by applying the operation C_3 on the components $(|\eta_1|, i|\eta_2|, 0)$ or directly on the gap function. The second domain we consider is when the nodes are in the $k_x k_z$ -plane. Then the B phase has order parameter components $(i|\eta_2|, 0, |\eta_1|)$ and the A phase has components $(0, 0, 1)$. Then the positions of the nodes are

$$\mathbf{k}_{F1} = \pm k_F (-\sin \phi_0 \hat{x} + \cos \phi_0 \hat{z}) \quad (42)$$

$$\mathbf{k}_{F2} = \pm k_F (\sin \phi_0 \hat{x} + \cos \phi_0 \hat{z}) \quad (43)$$

and the Doppler shifts are

$$\alpha_1(\mathbf{r}) = \pm \frac{k_F}{2mr} [\sin \phi_0 \sin \epsilon \cos \beta + \cos \phi_0 \sin \beta] \quad (44)$$

$$\alpha_2(\mathbf{r}) = \pm \frac{k_F}{2mr} [-\sin \phi_0 \sin \epsilon \cos \beta + \cos \phi_0 \sin \beta] \quad (45)$$

In the average over the vortex unit cell $\langle \alpha_1^2(\mathbf{r}) - \alpha_2^2(\mathbf{r}) \rangle_H$ vanishes, and

$$\langle \alpha_1^2(\mathbf{r}) + \alpha_2^2(\mathbf{r}) \rangle_H \sim \frac{v_F^2}{R^2} \ln \left(\frac{R}{\xi_0} \right) [\sin^2 \phi_0 \sin^2 \epsilon + \cos^2 \phi_0]. \quad (46)$$

Then the B phase thermal conductivity is

$$\left\langle \frac{\delta \tilde{\kappa}(0, \mathbf{r})}{T} \right\rangle_H \sim k_B^2 \frac{v_F \Delta_0^2}{v_g^2 \Gamma_0} \frac{H}{H_{c2}} \ln \left(\frac{H_{c2}}{H} \right) [\sin^2 \phi_0 \sin^2 \epsilon + \cos^2 \phi_0] \begin{pmatrix} \sin^2 \phi_0 & 0 & 0 \\ 0 & 0 & 0 \\ 0 & 0 & \cos^2 \phi_0 \end{pmatrix} \quad (47)$$

and the A phase thermal conductivity is $\kappa_{zz} \sim \text{constant}$.

In the third domain the nodes are found in the $k_y k_z$ -plane

$$\mathbf{k}_{F1} = \pm k_F (\cos \phi_0 \hat{y} - \sin \phi_0 \hat{z}) \quad (48)$$

$$\mathbf{k}_{F2} = \pm k_F (\cos \phi_0 \hat{y} + \sin \phi_0 \hat{z}) \quad (49)$$

In the average over the vortex unit cell, $\alpha_1^2(\mathbf{r}) - \alpha_2^2(\mathbf{r})$ again vanishes, and we find

$$\langle \alpha_1^2(\mathbf{r}) + \alpha_2^2(\mathbf{r}) \rangle_H \sim \frac{v_F^2}{R^2} \ln \left(\frac{H_{c2}}{H} \right) [\sin^2 \phi_0 + \cos^2 \phi_0 \cos^2 \epsilon]. \quad (50)$$

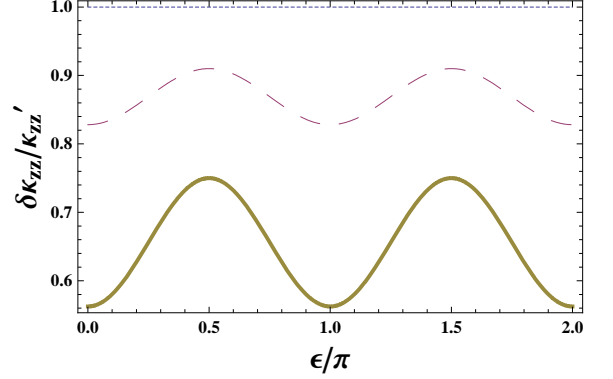


FIG. 2: (Color online) κ_{zz} (Eq. 47) for different values of ϕ_0 as a function of the field angle ϵ . The dotted line is for $\phi_0 = 0$ (A phase), the dashed line for $\phi_0 = \arcsin(0.3)$ and the bold one is for $\phi_0 = \frac{\pi}{6}$. $(\kappa'_{zz}/T) \sim k_B^2 \frac{v_F \Delta_0^2}{v_g^2 \Gamma_0} \frac{H}{H_{c2}} \ln \left(\frac{H_{c2}}{H} \right)$.

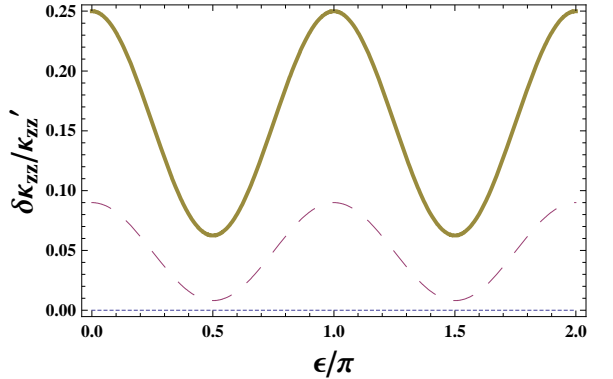


FIG. 3: (Color online) κ_{zz} (Eq. 51) for different values of ϕ_0 as a function of the field angle ϵ . The dotted line is for $\phi_0 = 0$ (A phase), the dashed line for $\phi_0 = \arcsin(0.3)$ and the bold one is for $\phi_0 = \frac{\pi}{6}$. $(\kappa'_{zz}/T) \sim k_B^2 \frac{v_F \Delta_0^2}{v_g^2 \Gamma_0} \frac{H}{H_{c2}} \ln \left(\frac{H_{c2}}{H} \right)$.

Then the B phase thermal conductivity is

$$\left\langle \frac{\delta \tilde{\kappa}(0, \mathbf{r})}{T} \right\rangle_H \sim k_B^2 \frac{v_F \Delta_0^2}{v_g^2 \Gamma_0} \frac{H}{H_{c2}} \ln \left(\frac{H_{c2}}{H} \right) \times [\sin^2 \phi_0 + \cos^2 \phi_0 \cos^2 \epsilon] \times \begin{pmatrix} 0 & 0 & 0 \\ 0 & \cos^2 \phi_0 & 0 \\ 0 & 0 & \sin^2 \phi_0 \end{pmatrix} \quad (51)$$

and the only non-vanishing component in the A phase is $\kappa_{yy} \sim \cos 2\epsilon$.

Domain averaging

In real situations, one may expect that either a single domain will form either because of sample shape or applied strains or fields, or that all three domains will be present. If all three domains are present then detailed knowledge of the domain structure is required to calcu-

late the conductivity. Lacking such knowledge, we consider two limiting cases: *i*) serial domains and *ii*) parallel domains. When the domains are in series the conductivity is $\tilde{\kappa} = (\tilde{\kappa}_1^{-1} + \tilde{\kappa}_2^{-1} + \tilde{\kappa}_3^{-1})^{-1}$ which vanishes in all components. When the domains are in parallel the three conductivities are simply added:

$$\left\langle \frac{\delta\tilde{\kappa}(0, \mathbf{r})}{T} \right\rangle_H \sim \begin{pmatrix} \sin^2 \epsilon (1 - \frac{3}{4} \sin^2 2\phi_0) + \frac{1}{2} \sin^2 2\phi_0 & -\frac{1}{4} \sin^2 \phi_0 \sin 2\epsilon & 0 \\ -\frac{1}{4} \sin^2 2\phi_0 \sin 2\epsilon & \cos^2 \epsilon (1 - \frac{3}{4} \sin^2 2\phi_0) + \frac{1}{2} \sin^2 2\phi_0 & 0 \\ 0 & 0 & 1 - \sin^2 \phi_0 \cos^2 \phi_0 \end{pmatrix} \quad (52)$$

for the B phase, while the result for the A phase ($\phi_0 = 0$) is

$$\left\langle \frac{\delta\tilde{\kappa}(0, \mathbf{r})}{T} \right\rangle_H \sim \begin{pmatrix} \sin^2 \epsilon & 0 & 0 \\ 0 & \cos^2 \epsilon & 0 \\ 0 & 0 & 1 \end{pmatrix} \quad (53)$$

Also, the domain averaged density of states is constant (has no oscillations).

Other nodal configurations

According to Table I of Ref. 54⁶¹ there are other nodal configurations corresponding to other superconducting phases which should be considered. Superconducting phases with cusp point nodes in tetrahedral superconductors are summarised in Table I.

Nodes	Symmetry	IR	channel
4 nodes $[0, \cos \phi_0, \pm \sin \phi_0]$	$D_2(E)$	T_u	triplet
2 nodes $[0, 0, 1]$	$D_2(C_2) \times \mathcal{K}, C_3(E)$	T_u	triplet
6 nodes $[0, 0, 1]$	$C_3 \times \mathcal{K}, C_2'(E), \mathcal{K}, E$	T_g	singlet
2 nodes $[1, 1, 1]$	$C_2(E) \times \mathcal{K}$	T_u	triplet
8 nodes $[1, 1, 1]$	$T(D_2), D_2 \times \mathcal{K}, D_2$	E_g	singlet
8 nodes $[1, 1, 1]$	$T(D_2)$	E_u	triplet
6 nodes $[0, 0, 1]$ and 2 nodes $[1, 1, 1]$	$C_3(E)$	T_g	singlet

TABLE I: Cusp point nodal configurations, their associated symmetries, order parameters labeled by irreducible representation (IR) and pairing channels for a tetrahedral superconductor (after Ref. 54).

For **eight point nodes in the [111] directions**, the thermal conductivity is

$$\left\langle \frac{\delta\tilde{\kappa}(0, \mathbf{r})}{T} \right\rangle_H \sim \begin{pmatrix} 2 & -\sin 2\epsilon & 0 \\ -\sin 2\epsilon & 2 & 0 \\ 0 & 0 & 2 \end{pmatrix} \quad (54)$$

The thermal conductivity for **two point nodes in the [111] directions** is

$$\left\langle \frac{\delta\tilde{\kappa}(0, \mathbf{r})}{T} \right\rangle_H \sim \left(1 - \frac{\sin 2\epsilon}{2}\right) \begin{pmatrix} 1 & 1 & 1 \\ 1 & 1 & 1 \\ 1 & 1 & 1 \end{pmatrix}. \quad (55)$$

Such a phase has three other domains, each with a single pair of nodes in the directions $[1 - 1 - 1]$, $[-11 - 1]$ and $[-1 - 11]$; the parallel domain averaged conductivity is equivalent to (54).

The thermal conductivity for **six point nodes in the [100] directions** is given by (53).

The thermal conductivity for **six point nodes in the [100] directions and two point nodes in the [111] directions** is given by the sum of (53) and (55). Such a phase has four domains; the parallel domain averaged conductivity is given by the sum of (53) and (54).

Eqs. 41, 47 and 51-55 are summarized in Table II. In all cases, the highest harmonics which appear are two-fold oscillations, stemming from the fact that contributions from pairs of nodes are additive and proportional to the square of the Doppler shift.

IV. DISCUSSION

So far there has only been one report of thermal conductivity in a rotating magnetic field, namely the results by Izawa *et al.*,³⁰ who measured κ_{zz} and found four-fold oscillations near H_{c2} and a sharp transition to two-fold oscillations at a lower field. We do not obtain four-fold oscillations for any of the point node configurations we considered and so we conclude that the formalism we have used is inapplicable in large magnetic fields. One possible source of error is that we have omitted contributions from quasi-particle states localised in vortex cores, and that these states may dominate the oscillatory contribution to the density of states as the field increases and the vortices become closer together. Another possibility is higher order in $\alpha(\mathbf{r})$ (the Doppler shift) contributions

Nodes	κ_{xx}	κ_{yy}	κ_{xy}	$\kappa_{xz,yz}$	κ_{zz}
4 nodes $[\cos \phi_0, \pm \sin \phi_0, 0]$	c	c	s	0	0
4 nodes $[\pm \sin \phi_0, 0, \cos \phi_0]$	c	0	0	0	c
4 nodes $[0, \cos \phi_0, \pm \sin \phi_0]$	0	c	0	0	c
domain average	c	c	s	0	1
2 nodes $[1, 0, 0]$	c	0	0	0	0
2 nodes $[0, 1, 0]$	0	c	0	0	0
2 nodes $[0, 0, 1]$	0	0	0	0	1
domain average/ 6 nodes $[1, 0, 0]$	c	c	0	0	1
2 nodes $[1, 1, 1]$	s	s	s	s	s
domain average/ 8 nodes $[1, 1, 1]$	1	1	s	0	1
6 nodes $[1, 0, 0]$ and 2 nodes $[1, 1, 1]$	c+s	c+s	s	s	s
domain average	c	c	s	0	1

TABLE II: Oscillatory contributions to the thermal conductivity with a field rotating in the xy plane for various nodal configurations. ‘s’ stands for $\sin 2\epsilon$, ‘c’ stands for $\cos 2\epsilon$, ‘1’ stands for no oscillations and ‘0’ means that the component vanishes. ϵ is the angle of the field with respect to the x axis.

become important as the field is increased. We do not obtain four-fold oscillations simply because we did not retain contributions to the density of states and thermal conductivity for powers of $\alpha(\mathbf{r})$ higher than two. In any case, unlike $d_{x^2-y^2}$ line node superconductors, the four-fold oscillations reported in Ref. 30 are not related in any simple way to the nodal structure of $\text{PrOs}_4\text{Sb}_{12}$.

Our results may be applicable to the lower field thermal conductivity measurements in which two-fold oscillations are found. The lower inset of Fig. 1 of Ref. 30 shows a nearly linear dependence of κ_{zz} on H , in rough agreement with $H \log H$ dependence expected for point nodes (see Eq. 41). Fig. 2b) of Ref. 30 clearly shows two-fold oscillations of the form $\kappa_{zz} \sim \cos 2\epsilon$ and *not* $\sin 2\epsilon$. This indicates that the most likely superconducting phase of $\text{PrOs}_4\text{Sb}_{12}$ is $D_2(E)$ which belongs to the three dimensional order parameter T_u and that a single domain with order parameter components $(0, |\eta_1|, i|\eta_2|)$ or $(i|\eta_2|, 0, |\eta_1|)$ was measured in Ref. 30. We note that this phase agrees with various properties observed in other experiments, including triplet pairing,⁴⁸ broken time reversal symmetry⁴¹ and broken C_3 symmetry.^{45,62}

Sakakibara et al.⁴⁰ measured the field-angle dependent specific heat and found four-fold oscillations, but unlike Izawa et al., no four-fold to two-fold transition was observed. In this case we must also attribute the four-fold oscillations to corrections beyond the semi-classical methods we have used. Sakakibara et al.⁴⁰ verified that, in their set-up, superconductivity has no preferred orientation, implying that their results are domain averaged. Since two-fold oscillations are not observed at all, these results may be consistent with any of the domain averaged configurations shown in Table II.

Similarly to computational issues pertaining to domain averaging, the thermal conductivity must also be aver-

aged over the vortex lattice. In all of our calculations we performed the vortex average as a simple areal average over a plane perpendicular to a vortex, as shown in Eq. 11. This procedure is appropriate when the heat current is parallel to the vortices. For currents in other directions a different averaging procedure should be used, which results in a more complicated field dependence of the oscillation amplitudes than what we have shown here. The correct procedure is an average of κ over paths through the vortex lattice, which is in fact more involved than the series average $\langle \kappa^{-1} \rangle^{-1}$ described in Ref. 7. This means that the vortex averaging calculation for any in-plane component of the conductivity will vary with the field angle, producing oscillations $\sim \cos 2\epsilon$ which are unrelated to nodes and which will dominate over any nodal contributions.^{32,63} Thus observations of oscillations $\sim \cos 2\epsilon$ in κ_{xx} , κ_{yy} or in off-diagonal components of κ measured with an in-plane current should not be interpreted as evidence of nodes.

For κ_{zz} , κ_{xz} and κ_{yz} , when the current is perpendicular to vortices, there will not be oscillations due to the vortex averaging. If observed, oscillations may therefore be attributed to nodes. A small oscillatory contribution will arise from mixing with the other components of κ via the vortex averaging procedure (which in general does involve averaging κ^{-1}) but we expect it to be small compared to the oscillations originating from nodes.

V. SUMMARY

We have reviewed previous works concerning field-angle dependent DOS and thermal conductivity for line node superconductors using a semi-classical method, and applied the same method to point node superconductors. This method neglects vortex localised quasi-particles and retains only the contribution from extended, nodal quasi-particles to the density of states. Clearly there are limitations to this approach; in particular it cannot be expected to produce an accurate estimate of the total low-energy density of states in point node superconductors. However it may be a reasonable way to estimate the field-angle dependent oscillatory component of the density of states and related quantities for fields $H_{c1} \leq H \ll H_{c2}$. We find that in point node superconductors there is no difference between the clean and dirty limits, unlike in line node superconductors in which the different limits produce significantly different expressions for the oscillatory part of the thermal conductivity. Considering all possible configurations of point nodes in a tetrahedral superconductor, we find that the superconducting phase $D_2(E)$, which we previously proposed based on other experimental evidence, best accounts for field-angle dependent oscillations in the thermal conductivity of $\text{PrOs}_4\text{Sb}_{12}$.

Acknowledgments

We thank Ilya Vekhter for helpful discussions. We gratefully acknowledge the hospitality of the University

of Waterloo, where this work was completed. This work was supported by NSERC of Canada.

-
- ¹ G. E. Volovik, JETP Lett. **58**, 469 (1993).
 - ² C. Caroli, P. G. de Gennes, and J. Matricon, Phys. Lett. **9**, 307 (1964).
 - ³ Y. S. Barash and A. A. Svidzinsky, Phys. Rev. B **53**, 15254 (1996); *ibid* **58**, 6476 (1998); *ibid* JETP Lett. **63**, 365 (1996)
 - ⁴ Y. S. Barash, A. A. Svidzinsky and V. P. Mineev, JETP Lett. **65**, 638 (1997).
 - ⁵ P. J. Hirschfeld, J. Korean Phys. Soc. **33**, 485 (1998).
 - ⁶ C. Kübert and P. J. Hirschfeld, Solid State Commun. **105**, 459 (1998).
 - ⁷ C. Kübert and P. J. Hirschfeld, Phys. Rev. Lett. **80**, 4963 (1998).
 - ⁸ I. Vekhter, J. P. Carbotte and E. J. Nicol, Phys. Rev. B **59**, 1417 (1999).
 - ⁹ M. Franz, Phys. Rev. Lett. **82**, 1760 (1999).
 - ¹⁰ I. Vekhter and A. Houghton, Phys. Rev. Lett. **83**, 4626 (1999).
 - ¹¹ I. Vekhter and P. J. Hirschfeld, Physica C **341-348**, 1947 (2000).
 - ¹² K. A. Moler, A. Kapitulnik, D. J. Baar, R. Liang, and W. N. Hardy, Phys. Chem. Solids **56**, 1899 (1995).
 - ¹³ K. A. Moler, D. L. Sisson, J. S. Urbach, M. R. Beasley, A. Kapitulnik, D. J. Baar, R. Liang, and W. N. Hardy, Phys. Rev. B **55** 3954 (1997).
 - ¹⁴ I. Vekhter, P. J. Hirschfeld, J. P. Carbotte and E. J. Nicol, Phys. Rev. B **59**, R9023 (1999).
 - ¹⁵ I. Vekhter, P. J. Hirschfeld and E. J. Nicol, Phys. Rev. B **64**, 064513 (2001)
 - ¹⁶ H. Won and K. Maki, Europhys. Lett. **56**, 729 (2001).
 - ¹⁷ P. Miranović, N. Nakai, M. Ichioka, and K. Machida, Phys. Rev. B **68**, 052501 (2003).
 - ¹⁸ M. Udagawa, Y. Yanase, and M. Ogata, Phys. Rev. B **70**, 184515 (2004).
 - ¹⁹ P. Thalmeier, T. Watanabe, K. Izawa, and Y. Matsuda, Phys. Rev. B **72**, 024539 (2005).
 - ²⁰ L. Tewordt and D. Fay, Phys. Rev. B **72**, 014502 (2005).
 - ²¹ A. Vorontsov and I. Vekhter, Phys. Rev. Lett. **96**, 237001 (2006).
 - ²² A. Vorontsov and I. Vekhter Phys. Rev. B **75**, 224501 (2007).
 - ²³ A. Vorontsov and I. Vekhter Phys. Rev. B **75**, 224502 (2007).
 - ²⁴ H. Aubin, K. Behnia, M. Ribault, R. Gagnon and L. Taillefer, Phys. Rev. Lett. **78**, 2624 (1997).
 - ²⁵ F. Yu, M. B. Salamon, A. J. Leggett, W. C. Lee, and D. M. Ginsberg, Phys. Rev. Lett. **74**, 5136 (1995).
 - ²⁶ K. Izawa, H. Takahashi, H. Yamaguchi, Y. Matsuda, M. Suzuki, T. Sasaki, T. Fukase, Y. Yoshida, R. Settai, and Y. Onuki, Phys. Rev. Lett. **86**, 2653 (2001).
 - ²⁷ K. Izawa, H. Yamaguchi, Yuji Matsuda, H. Shishido, R. Settai, and Y. Onuki, Phys. Rev. Lett. **87**, 057002 (2001).
 - ²⁸ K. Izawa, H. Yamaguchi, T. Sasaki, and Y. Matsuda, Phys. Rev. Lett. **88**, 027002 (2001).
 - ²⁹ K. Izawa, K. Kamata, Y. Nakajima, Y. Matsuda, T. Watanabe, M. Nohara, H. Takagi, P. Thalmeier, and K. Maki, Phys. Rev. Lett. **89**, 137006 (2002).
 - ³⁰ K. Izawa, Y. Nakajima, J. Goryo, Y. Matsuda, S. Osaki, H. Sugawara, H. Sato, P. Thalmeier, and K. Maki, Phys. Rev. Lett. **90**, 117001 (2003).
 - ³¹ T. Watanabe, K. Izawa, Y. Kasahara, Y. Haga, Y. Onuki, P. Thalmeier, K. Maki, and Y. Matsuda, Phys. Rev. B **70**, 184502 (2004).
 - ³² Y. Matsuda, K. Izawa, and I. Vekhter, J. Phys.: Condens. Matter **18**, R705 (2006).
 - ³³ T. Park, M. Salamon, E. Choi, H. Kim, and S. Lee, Phys. Rev. Lett. **90**, 177001 (2003).
 - ³⁴ T. Park, E. Chia, M. Salamon, E. Bauer, I. Vekhter, J. Thompson, E. Choi, H. Kim, S. Lee, and P. Canfield, Phys. Rev. Lett. **92**, 237002 (2004).
 - ³⁵ K. Deguchi, Z. Q. Mao, H. Yaguchi, and Y. Maeno, Phys. Rev. Lett. **92**, 047002 (2004).
 - ³⁶ K. Deguchi, Z. Q. Mao, and Y. Maeno, J. Phys. Soc. Jpn. **73** 1313 (2004).
 - ³⁷ H. Aoki, T. Sakakibara, H. Shishido, R. Settai, Y. Onuki, P. Miranović and K. Machida, J. Phys.: Condens. Matter **16**, L13 (2004).
 - ³⁸ J. Custers, Y. Namai, T. Tayama, T. Sakakibara, H. Sugawara, Y. Aoki, and H. Sato, Physica B **378-380**, 179 (2006).
 - ³⁹ J. Custers, A. Yamada, T. Tayama, T. Sakakibara, H. Sugawara, Y. Aoki, H. Sato, Y. Onuki, and K. Machida, J. Magn. Magn. Mater. **310**, 700 (2007).
 - ⁴⁰ T. Sakakibara, A. Yamada, J. Custers, K. Yano, T. Tayama, H. Aoki, and K. Machida, J. Phys. Soc. Jpn. **76**, 051004 (2007).
 - ⁴¹ Y. Aoki, A. Tsuchiya, T. Kanayama, S. R. Saha, H. Sugawara, H. Sato, W. Higemoto, A. Koda, K. Ohishi, K. Nishiyama, and R. Kadono, Phys. Rev. Lett. **91**, 067003 (2003).
 - ⁴² M. B. Maple, E. D. Bauer, V. S. Zapf, E. J. Freeman, N. A. Frederick, and R. P. Dickey, Acta Phys. Pol. B **32**, 3291 (2001).
 - ⁴³ E. D. Bauer, N. A. Frederick, P.-C. Ho, V. S. Zapf, and M. B. Maple, Phys. Rev. B **65**, 100506(R) (2002).
 - ⁴⁴ E. E. M. Chia, M. B. Salamon, H. Sugawara, and H. Sato, Phys. Rev. Lett. **91**, 247003 (2003).
 - ⁴⁵ A. D. Huxley, M.-A. Measson, K. Izawa, C. D. Dewhurst, R. Cubitt, B. Grenier, H. Sugawara, J. Flouquet, Y. Matsuda, and H. Sato, Phys. Rev. Lett. **93**, 187005 (2004).
 - ⁴⁶ M. Nishiyama, T. Kato, H. Sugawara, D. Kikuchi, H. Sato, H. Harima, and G.-q. Zheng, J. Phys. Soc. Jpn. **74**, 1938 (2005).
 - ⁴⁷ N. A. Frederick, T. A. Sayles and M. B. Maple, Phys. Rev. B **71**, 064508 (2005).
 - ⁴⁸ W. Higemoto, S. R. Saha, A. Koda, K. Ohishi, R. Kadono, Y. Aoki, H. Sugawara and H. Sato, Phys. Rev. B **75**, 020510(R) (2007).
 - ⁴⁹ K. Katayama, S. Kawasaki, M. Nishiyama, H. Sugawara, D. Kikuchi, H. Sato, and G.-q. Zheng, J. Phys. Soc. Jpn.

- 76**, 023701 (2007).
- ⁵⁰ G. Seyfarth, J. P. Brison, M.-A. Méasson, D. Braithewaite, G. Lapertot and J. Flouquet, *Phys. Rev. Lett.* **97**, 236403 (2006).
- ⁵¹ D. E. MacLaughlin, J. E. Sonier, R. H. Heffner, O. O. Bernal, B.-L. Young, M. S. Rose, G. D. Morris, E. D. Bauer, T. D. Do and M. B. Maple, *Phys. Rev. Lett.* **89**, 157001 (2002).
- ⁵² H. Suderow, S. Viera, J. D. Strand, S. Bud'ko and P. C. Canfield, *Phys. Rev. B* **69**, 060504 (2004).
- ⁵³ H. Kotegawa, M. Yogi, Y. Imamura, Y. Kawasaki, G.-q. Zheng, Y. Kitaoka, S. Ohsaki, H. Sugawara, Y. Aoki, and H. Sato, *Phys. Rev. Lett.* **90**, 027001 (2003).
- ⁵⁴ I. A. Sergienko and S. H. Curnoe, *Phys. Rev. B*, **70**, 144522 (2004).
- ⁵⁵ T. R. Abu Alrub and S. H. Curnoe, *Phys. Rev. B* **76**, 054514 (2007).
- ⁵⁶ C. J. Pethick and D. Pines, *Phys. Rev. Lett.* **57**, 118 (1986).
- ⁵⁷ A slight error in Ref. 7 has been corrected here.
- ⁵⁸ G. D. Mahan, *Many-Particle Physics* (Plenum Press, 3rd edition, New York) (2000).
- ⁵⁹ A. C. Durst and P. A. Lee, *Phys. Rev. B* **62**, 1270 (2000).
- ⁶⁰ T. R. Abu Alrub and S. H. Curnoe, *Phys. Rev. B* **76**, 184511 (2007).
- ⁶¹ An error in Table I of Ref. 54, which stated that there are no nodes in the $(|\eta_1|, i|\eta_2|, 0)$ triplet phase was corrected in Ref. 55.
- ⁶² S. Mukherjee and D. F. Agterberg, *Phys. Rev. B* **74**, 174505 (2006).
- ⁶³ K. Maki, *Phys. Rev.* **158**, 397 (1967).
- ⁶⁴ In Ref. 55 we incorrectly stated that there were 6 domains with 6 different nodal structures associated with $(|\eta_1|, i|\eta_2|, 0)$. There in fact only three different nodal structures.